PHYSICAL REVIEW B, VOLUME 65, 100403(R)

Magnetic versus orbital polarons in colossal magnetoresistance manganites

J. M. De Teresa, M. R. Ibarra, P. Algarabel, L. Morellon, B. García-Landa, and C. Marquina
Magnetismo de Sólidos, Instituto de Ciencia de Materiales de Aragón, CSIC-Universidad de Zaragoza, Facultad de Ciencias, 50009 Zaragoza, Spain

C. Ritter
Institut Laue Langevin, Boîte Postale 156, F-38042 Grenoble Cedex 9, France

A. Maignan, C. Martin, and B. Raveau
Laboratoire Crismat, Ismra, Boulevard du Mal Juin, 140050 Caen Cedex, France

A. Kurbakov and V. Trounov
Physics Institute, Orlova Grove, Gatchina, Leningrad district, 188350 Russia
(Received 18 December 2001; published 12 February 2002)

In order to investigate the paramagnetic ground state of the colossal magnetoresistance (CMR) $Sm_{0.55}Sr_{0.45}MnO_3$ compound we have used a wide set of techniques: magnetoresistance, magnetization, high-resolution neutron diffraction, small-angle neutron diffraction, and muon spin relaxation. According to these measurements the paramagnetic ground state would consist of ~0.8 nm ferromagnetic clusters embedded in a short-range charge/orbital ordered matrix. The CMR effect occurs due to percolation of these ferromagnetic clusters.

DOI: 10.1103/PhysRevB.65.100403 PACS number(s): 75.30.Vn, 61.12.Ex, 75.30.Cr, 76.75.+i

Colossal magnetoresistance (CMR), i.e., a change in resistance of several orders of magnitude by applying a magnetic field, in perovskite manganites ($AA'MnO_3$) is currently a hot topic in magnetism.[1,2] From a fundamental point of view, the central question is to identify the mechanisms responsible for the existence of CMR. For example, CMR can occur if the application of a magnetic field causes the melting of a long-range charge/orbital-ordered ground state,[3] or a change in the relative fraction of coexisting microscopic (~500 nm) metallic long-range ferromagnetic and insulating long-range charge/orbital-ordered domains.[4] There is an additional mechanism that occurs in the paramagnetic phase of certain compounds like $La_{2/3}Ca_{1/3}MnO_3$,[5–8] and $Sm_{0.55}Sr_{0.45}MnO_3$,[9–11] which is the aim of the present study.

In the case of $La_{2/3}Ca_{1/3}MnO_3$, a behavior characteristic of charge localization and short-range ferromagnetic order was observed in the paramagnetic phase and interpreted as due to charge localization within a ferromagnetic cloud of ~1.2 nm extent, i.e., a magnetic polaron.[5] As the first electron diffraction experiments did not report any signature of charge ordering in this compound,[12] it seemed natural to consider the charge to be confined within the magnetic polarons. However, recent electron diffraction as well as neutron diffraction experiments point to the existence of short-range charge/orbital ordering in the paramagnetic phase of this compound.[6,8] In order to explain the simultaneous presence of short-range ferromagnetic and charge/orbital ordering, some authors have proposed that the short-range ferromagnetic correlation might correspond to small ferromagnetic segments in the CE-type charge/orbital ordering.[7] This issue is crucial in order to understand the ground state of this compound and the origin of the CMR. $Sm_{0.55}Sr_{0.45}MnO_3$ is another archetypal CMR compound that has recently attracted much attention due to the strong competition between the ferromagnetic and charge/orbital ordered ground states. At $T_C \sim 120$ K this compound orders ferromagnetically and above T_C, a strong *x*-ray diffuse scattering has been observed below 300 K and assigned to short-range CE-type charge/orbital ordering.[9,10] We have investigated this compound with several experimental techniques and, as discussed hereafter, our results are consistent with a paramagnetic ground state consisting of ~0.8 nm ferromagnetic clusters embedded in a short-range charge/orbital ordered matrix. *The CMR effect would occur due to percolation of these ferromagnetic clusters where the charge is delocalized.*

The samples used in these experiments are polycrystalline and have been prepared by standard solid state procedures. X-ray diffraction patterns at room temperature have been fitted with the FULLPROF program within the orthorhombic *Pnma* space group with lattice parameters: $a = 5.422(1)$ Å, $b = 7.6765(5)$ Å, $c = 5.4277(8)$ Å. For the neutron experiments, and in order to minimize the neutron absorption of Sm, the compound was synthesized with ^{152}Sm. *Magnetoresistance measurements* have been performed with the four-probe technique and are shown in Fig. 1. Above $T_C \sim 120$ K, the compound is semiconducting and becomes metallic-like below this temperature. The residual resistance is high due to the polycrystalline nature of the sample and, consequently, there is a strong contribution from spin-polarized transport through the grain boundaries. Below T_C, the observed magnetoresistance is assigned to tunnel magnetoresistance through the grain boundaries.[13] By applying a magnetic field of several tesla, the CMR effect is observed in the paramagnetic phase. The transition is strongly hysteretic at zero field as can be observed in the inset of Fig. 1 and suggests that the transition is of *first order*. However, at 7 T the hysteresis has disappeared or is very small. This could

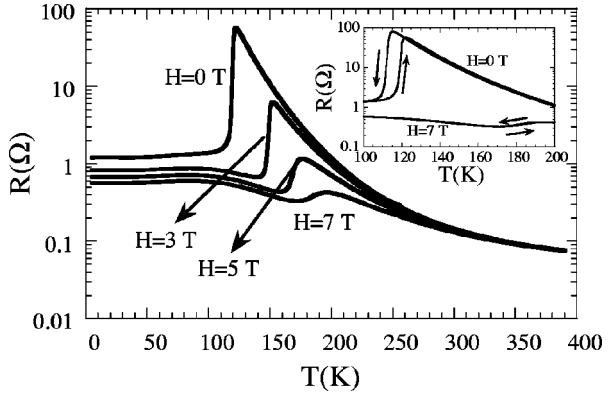

FIG. 1. Resistance as a function of temperature (data taken by heating) of $Sm_{0.55}Sr_{0.45}MnO_3$ under magnetic fields of 0, 3, 5, and 7 T. The inset shows the resistance when cooling and heating at 0 and 7 T.

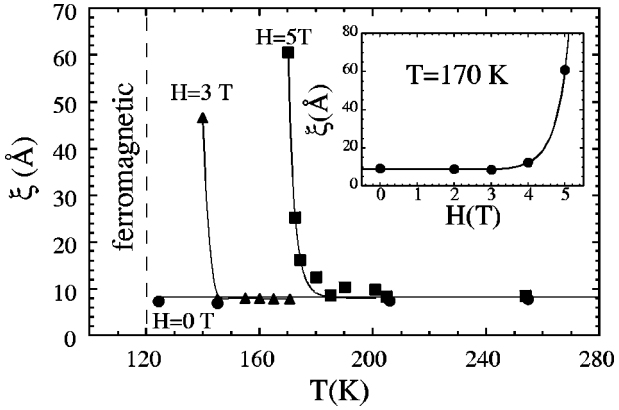

FIG. 2. Magnetic correlation length of $Sm_{0.55}Sr_{0.45}MnO_3$ as a function of the temperature and under magnetic fields of 0, 3, and 5 T (see text). The inset shows the dependence of the magnetic correlation length with the magnetic field at 170 K.

mean that under a large magnetic field the transition becomes of *second-order* as predicted by some CMR theories.[2]

High-resolution neutron diffraction experiments have been performed at the Institut Laue-Langevin (ILL), located in Grenoble (France) by using the high-intensity powder diffractometer D2B, with neutron wavelength $\lambda = 1.6$ Å. Data were taken at three selected temperatures: at 400 K, 135 K, and 4 K. The data were analyzed using the Rietveld refinement program FULLPROF. A very small amount of the impurity Mn_3O_4 has been detected. The important results extracted from these measurements are the following. First, at the three temperatures the data can be well fitted with only one orthorhombic *Pnma* crystallographic structure. Second, in the paramagnetic phase at 135 K (i.e., ~15 K above T_C) there is no magnetic contribution and no sign of long-range charge/orbital ordering. At 4 K (i.e., below T_C), the data can be well fitted with a homogeneous ferromagnetic phase and the magnetic moment per Mn ion is $\sim 3.4\mu_B$, which is very close to the expected value for full ferromagnetic alignment ($3.55\mu_B$). We can conclude that the CMR observed in $Sm_{0.55}Sr_{0.45}MnO_3$ is not due to the existence of either a long-range charge/orbital-ordered ground state or micrometric phase segregation.

In order to investigate the magnetic correlations in the paramagnetic phase, we have carried out *small-angle neutron scattering (SANS) measurements* at ILL. The experiments were performed at the instrument D16 with neutron wavelength $\lambda = 4.5$ Å and momentum transfer $0.04\ \text{Å}^{-1} \leqslant q \leqslant 0.6\ \text{Å}^{-1}$ (resolution $\Delta q = 0.005\ \text{Å}^{-1}$) across the temperature range $4\ \text{K} \leqslant T \leqslant 300$ K and with magnetic fields up to 5 T. Assuming ferromagnetic correlations of the Ornstein-Zernike type $\langle M(0) \cdot M(r) \rangle \sim [\exp(-r/\xi)]/r$, where ξ is the ferromagnetic correlation length, the SANS intensity should behave as $I = I_0/[q^2 + (1/\xi)^2]$, i.e., Lorentzian dependence.[14] After subtracting the incoherent nuclear scattering, we have obtained the magnetic SANS. This scattering is strong in the paramagnetic phase and collapses at the transition to the ferromagnetic phase, which *indicates the presence in the paramagnetic phase of ferromagnetic clusters that are stable longer than ~1 ps*. The SANS intensity has been fitted to $I = I_0/[q^2 + (1/\xi)^2]$ and ξ has been extracted.

In Fig. 2 the values of ξ are shown as a function of temperature under magnetic fields of 0, 3, and 5 T. Without applied magnetic field, one can notice that ξ is ≈ 0.8 nm in the paramagnetic phase. Below T_C, the magnetic SANS intensity is zero. This means that in the paramagnetic phase well-defined ferromagnetic clusters of size around 0.8 nm exist. We have measured some isotherms just above T_C in order to monitor the evolution of ξ with the magnetic field. However, the transition is so abrupt that it has not been possible to get any intermediate state between the 0.8-nm-cluster regime and the ferromagnetic regime. This correlates with the fact that the transition is of first-order type as discussed previously. However, we have mentioned that the transition becomes continuous under high magnetic fields. Thus, under applied magnetic fields of 3 and 5 T it has been possible to get intermediate states with clusters of $\xi > 0.8$ nm as shown in Fig. 2. Also, intermediate states are obtained in an isotherm at 170 K (see inset of Fig. 2). One can notice that *ξ increases with the magnetic field*. It means that the ferromagnetic clusters increase in size and finally percolate to produce the long-range ferromagnetic state (this has been monitored by studying the field dependence of a Bragg magnetic peak). As a consequence, the ferromagnetic clusters that we observe should not be the same as the charge-ordered/orbital clusters detected with x-ray diffuse scattering, whose size should decrease with the magnetic field. If their size increased, a long-range charge-ordered/orbital state would realize, which is not the case.

The existence of strong short-range magnetic interactions in the paramagnetic phase can be also inferred from the *magnetization measurements* shown in Fig. 3. These experiments have been performed with a SQUID magnetometer under 0.01 T, 3 T, and 5 T across the temperature range $4\ \text{K} \leqslant T \leqslant 400$ K. Under 0.01 T, the ferromagnetic transition, T_C, occurs at around 120 K and the low value of the magnetization is consistent with a saturation field larger than 0.01 T. Under 3 T and 5 T, the magnetic domain structure has already disappeared and we measure the full saturation magnetization, $\sim 3.4\mu_B$. We have fitted the data above T_C to a Curie-Weiss law: $H/M = (T - \Theta)/C$, where C is the Curie

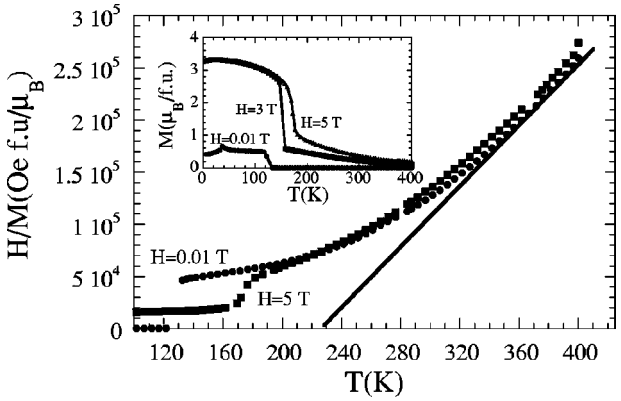

FIG. 3. Experimental data of the inverse susceptibility as a function of temperature under 0.01 T (dots) and 5 T (squares) and expected behavior in the case of free paramagnetic Mn ions (straight line). The inset shows the magnetization as a function of temperature under fields of 0.01 T, 3 T, and 5 T.

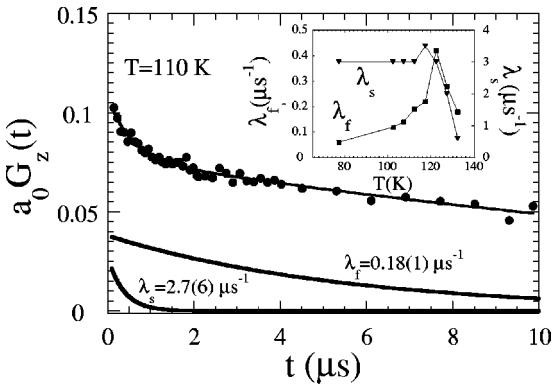

FIG. 4. Experimental data (dots) of the muon depolarization at 110 K of $Sm_{0.55}Sr_{0.45}MnO_3$ and corresponding fit (line) to the two-exponential function: $a_0G_z(t)=a_b+A_f\exp(-\lambda_f t)+A_s\exp(-\lambda_s t)$, where $a_b=0.045$, $A_f=0.038(2)$, $\lambda_f=0.18(1)\ \mu s^{-1}$, $A_s=0.028(4)$, and $\lambda_s=2.7(6)\ \mu s^{-1}$. It is also shown the relative contribution of each of these exponentials. In the inset, the values of the ''fast'' (squares) and ''slow'' (triangles) relaxation rates across the temperature interval $75\ K\leqslant T\leqslant 130\ K$ are shown.

constant, $C=(Np_{\rm eff}^2)/3K_B$ with N being the number of magnetic entities and $p_{\rm eff}$ the effective magnetic moment, $p_{\rm eff}^2=g^2S(S+1)\mu_B^2$. In the case of free paramagnetic ions the expected value of C is 4.4×10^{-4} K μ_B/f.u. Oe. The obtained experimental value is slightly higher at 400 K ($C=5.5\times10^{-4}$ K μ_B/f.u. Oe) and one order of magnitude higher at temperatures close to T_C ($C=4\times10^{-3}$ K μ_B/f.u. Oe). This is an indication of the existence of short-range magnetic order in the paramagnetic phase,[15] even though a realistic quantitative description of the inverse magnetization versus temperature is yet to be done.

The spin dynamics has also been investigated by means of *zero-field muon spin relaxation* (ZF-μSR) studies carried out at the ISIS pulsed muon facility (Rutherford Appleton Laboratory, UK) using the MuSR spectrometer. ZF-μSR measurements were carried out in a closed-cycle refrigerator using a 10-g powder sample mounted in a titanium sample holder and spectra were recorded on cooling. Longitudinal field measurements in a magnetic field of 100 Oe were performed at selected temperatures in the paramagnetic phase with no significant changes in the relaxation, thus excluding any additional nuclear static component. The results will be discussed within the scenario proposed by Heffner *et al.* in order to explain the μSR and neutron spin echo measurements in manganese perovskites.[16,17] μSR data can be normally fit to a relaxation function with two contributions $G_z(t)=A_{\rm osc}G_{\rm osc}(t)+A_{\rm rlx}G_{\rm rlx}(t)$ but due to the instrument resolution of MuSR spectrometer only the relaxing term $G_{\rm rlx}(t)$ was observed in our experiments. This term describes the local spin dynamics and in a typical magnetic material $G_{\rm rlx}(t)$ is given by an exponential function $A_{\rm rlx}\exp(-\lambda t)$ where $\lambda=1/T_1$ is the characteristic spin-lattice relaxation rate. However, Heffner *et al.* have found that in some ferromagnetic manganites ($La_{1-x}Ca_xMnO_3$) one needs a stretched exponential function or a two-exponential function in order to fit the experimental results.[16,17] This is thought to arise from inhomogeneous Mn spin dynamics. We find that our μSR data of $Sm_{0.55}Sr_{0.45}MnO_3$ can be satisfactorily fitted either to a stretched exponential or to a two-exponential relaxation function. First, we have fitted the μSR data in the whole temperature range (300 K–20 K) with a stretched exponential $a_0G_z(t)=a_b+A\exp[-(\lambda t)^\beta]$. The relaxation rate, λ, peaks at the ferromagnetic transition ($T_C=121$ K) following a temperature dependence above T_C of the form $\lambda(T)=\lambda_0(T/T_C-1)^{-\gamma}$, with $\lambda_0=0.102(3)\ \mu s^{-1}$, $T_C=121.3(2)$ K, and $\gamma=0.35(2)$. The effective initial asymmetry, A, in the ferromagnetic phase decreases to $\frac{1}{3}$ of its value in the paramagnetic phase, which is consistent with the onset of a ferromagnetic state. The β exponent is equal to 1 above 135 K (single exponential decay) and decreases to about 0.3 at low temperatures. The data can be also fit to a two-exponential relaxation function $a_0G_z(t)=a_b+A_f\exp(-\lambda_f t)+A_s\exp(-\lambda_s t)$, which, according to Heffner and coworkers, fits considerably better the experimental results of $La_{2/3}Ca_{1/3}MnO_3$.[17] This is interpreted as due to two spatially separated regions possessing very different Mn-ion spin dynamics. As a consequence, we suggest in $Sm_{0.55}Sr_{0.45}MnO_3$ the presence of two regions with ''fast'' and ''slow'' relaxation rates, respectively. This fit has been obtained successfully at the neighborhood of the transition temperature ($75\ K\leqslant T\leqslant 130$ K) as is displayed in Fig. 4. For temperatures below 75 K and above 130 K, either the overall relaxation rate is too small or the two exponentials cannot be resolved clearly. We propose that the two regions with ''fast'' and ''slow'' relaxation rates could correspond respectively to relaxation phenomena of the short-range ferromagnetic clusters and the short-range charge/orbital ordering matrix. In $La_{0.67}Ca_{0.33}MnO_3$, a similar analysis close to T_C (270 K) produces $\lambda_f\sim0.1\ \mu s^{-1}$ and $\lambda_s\sim1\ \mu s^{-1}$, which are similar values to those of $Sm_{0.55}Sr_{0.45}MnO_3$, and interpreted as due to Mn ion spin dynamics within conductive double-exchange ferromagnetic clusters and insulating regions respectively.[17]

In order to explain the CMR and the whole set of experimental results in the compound $Sm_{0.55}Sr_{0.45}MnO_3$ we propose the following scenario, which is schematized in Fig. 5. SANS measurements detect the existence of ferromagnetic

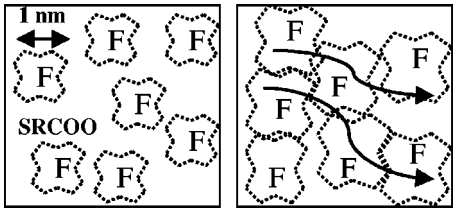

FIG. 5. Proposed scenario to explain the CMR in the paramagnetic phase of $Sm_{0.55}Sr_{0.45}MnO_3$. The ground state would consist of conductive short-range (~0.8 nm) ferromagnetic clusters embedded in an insulating short-range charge/orbital ordered (SRCOO) matrix, which produces a high-resistance state. By applying a magnetic field, percolation of these ferromagnetic clusters leads to a metallic state (CMR effect).

clusters above T_C with size ~0.8 nm that are stable longer than 1 ps. Several features support the fact that these clusters are of different nature than those observed with x-ray diffuse scattering in this compound. Our ferromagnetic clusters grow in size when applying a magnetic field whereas the magnetic field inhibits the CE-type ordering.[3] Moreover, we note that in the $La_{1-x}Ca_xMnO_3$ series, the strongest short-range ferromagnetic order occurs for $x \sim \frac{5}{8}$ whereas the strongest short-range charge/orbital order occurs for $x \sim \frac{1}{2}$.[7] This indicates that *both phenomena are not correlated*. The most plausible scenario in $Sm_{0.55}Sr_{0.45}MnO_3$ is that short-range ferromagnetic clusters form in a paramagnetic matrix that develops short-range charge/orbital correlations. The charge is delocalized within the ferromagnetic clusters but rather localized within the CE-type short-range charge/orbital ordered background. This would explain the overall semiconducting behavior of the resistance in the paramagnetic phase. The CMR effect occurs because when applying the magnetic field the ferromagnetic clusters grow and percolate, which short-circuits the current.[18] The muon depolarization data are also consistent with the existence of two spatially-separated regions having respectively a ''fast'' and a ''slow'' spin dynamics. The experimental microscopic behavior of $La_{2/3}Ca_{1/3}MnO_3$ is similar to that of $Sm_{0.55}Sr_{0.45}MnO_3$, which suggests that the same scenario can be applied to explain the CMR in both compounds. This is not a trivial result because $Sm_{0.55}Sr_{0.45}MnO_3$ was considered to be a CMR compound dominated by lattice effects in the paramagnetic phase and no role was assigned to the double-exchange ferromagnetic clusters.[10] Our work suggests that it is a general trend in manganites developing CMR in the paramagnetic phase that the competition between insulating charge/orbital ordering and conducting double-exchange interactions produces the coexistence of short-range entities of both types and this is at the origin of the CMR. This model is different from another proposed model in which the same entity (a magnetopolaron) produces at the same time the short-range magnetic and lattice effects.[5–7]

We acknowledge the Spanish CICYT for financial support as well as the EC financial aid for the μSR experiments at ISIS and the assistance of P.J.C. King during these experiments.

[1] J. M. D. Coey, M. Viret, and S. Von Molnar, Adv. Phys. **48**, 167 (1999).

[2] E. Dagotto, T. Hotta, and A. Moreo, Phys. Rep. **344**, 1 (2001).

[3] Y. Tokura and Y. Tomioka, J. Magn. Magn. Mater. **200**, 1 (1999).

[4] M. R. Ibarra, G-M Zhao, J. M. De Teresa, B. García-Landa, Z. Arnold, C. Marquina, P. A. Algarabel, H. Keller, and C. Ritter, Phys. Rev. B **57**, 7446 (1998); M. Uehara, S. Mori, C. H. Chen, and S-W. Cheong, Nature (London) **399**, 560 (1999).

[5] J. M. De Teresa, M. R. Ibarra, P. A. Algarabel, C. Ritter, C. Marquina, J. Blasco, J. García, A. del Moral, and Z. Arnold, Nature (London) **386**, 256 (1997); J. Lynn, R. W. Erwin, J. A. Borchers, Q. Huang, A. Santoro, J-L. Peng, and Z. Y. Li, Phys. Rev. Lett. **76**, 4046 (1996).

[6] C. P. Adams, J. W. Lynn, Y. M. Mukovskii, A. A. Arsenov, and D. A. Shulyatev, Phys. Rev. Lett. **85**, 3954 (2000); P. Dai, J. A. Fernandez-Baca, N. Wakabayashi, E. W. Plummer, Y. Tomioka, and Y. Tokura, *ibid.* **85**, 2553 (2000).

[7] K. H. Kim, M. Uehara, and S-W. Cheong, Phys. Rev. B **62**, R11 945 (2000).

[8] J. M. Zuo and J. Tao, Phys. Rev. B **63**, 060407 (2001); A. K. Pradhan, B. K. Roul, Y. Feng, Y. Wu, S. Mohanty, D. R. Sahu, and P. Dutta, Appl. Phys. Lett. **78**, 1598 (2001).

[9] Y. Tomioka, H. Kuwahara, A. Asamitsu, M. Kasai, and Y. Tokura, Appl. Phys. Lett. **70**, 3609 (1997); C. Martin, A. Maignan, M. Hervieu, and B. Raveau, Phys. Rev. B **60**, 12 191 (1999).

[10] Y. Tokura and N. Nagagosa, Science **288**, 462 (2000); E. Saitoh, Y. Tomioka, T. Kimura, and Y. Tokura, J. Phys. Soc. Jpn. **69**, 2403 (2000).

[11] A. I. Abramovich, L. I. Koroleva, A. V. Michurin, O. Y. Gorbenko, and A. R. Kaul, Physica B **293**, 38 (2000); C. Marquina, M. R. Ibarra, A. I. Abramovich, A. V. Michurin, and L. I. Koroleva, J. Magn. Magn. Mater. **226–230**, 999 (2001).

[12] C. H. Chen and S-W. Cheong, Phys. Rev. Lett. **76**, 4042 (1996).

[13] H. Y. Hwang, S-W. Cheong, N. P. Ong, and B. Batlogg, Phys. Rev. Lett. **77**, 2041 (1996).

[14] S. K. Burke, Cywinski, and B. Rainford, J. Appl. Crystallogr. **11**, 644 (1978).

[15] H. Yi, N. H. Hur, and J. Yu, Phys. Rev. B **61**, 9501 (2000); R. Borges, F. Ott, R. M. Thomas, V. Skumryev, J. M. D. Coey, J. I. Arnaudas, and L. Ranno, *ibid.* **60**, 12 847 (2000).

[16] R. H. Heffner, L. P. Le, M. F. Hundley, J. J. Neumeier, G. M. Luke, K. Kojima, B. Nachumi, Y. J. Uemura, D. E. MacLaughlin, and S-W. Cheong, Phys. Rev. Lett. **77**, 1869 (1996).

[17] R. H. Heffner, J. E. Sonier, D. E. MacLaughlin, G. J. Nieuwenhuys, G. Ehlers, F. Mezei, S.-W. Cheong, J. S. Gardner, and H. Röder, Phys. Rev. Lett. **85**, 3285 (2000); R. H. Heffner, J. E. Sonier, D. E. MacLaughlin, G. J. Nieuwenhuys, G. M. Luke, Y. J. Uemura, W. Ratcliff II, S-W. Cheong, and G. Balakrishnan, Phys. Rev. B **63**, 094408 (2001).

[18] M. Mayr, A. Moreo, J. A. Vergés, J. Arispe, A. Feiguin, and E. Dagotto, Phys. Rev. Lett. **86**, 135 (2001).